ISBN 82-553-0330-8
Applied Mathematics
No 3 - October 25 1977

ON THE STABILITY OF NON-LINEAR CONVECTION IN A HELE-SHAW CELL

by

Oddmund Kvernvold
Oslo

PREPRINT SERIES - Matematisk institutt, Universitetet i Oslo

ON THE STABILITY OF NON-LINEAR CONVECTION IN A HELE-SHAW CELL

by

Oddmund Kvernvold
Department of Mechanics
University of Oslo

Abstract

A numerical analysis of non-linear convection in a Hele-Shaw cell heated from below is performed. The stability of the stationary solutions with respect to infinitesimal disturbances are examined. Further, the velocity distribution in the convection cell is discussed, and the theoretical results are found to fit well with available experimental data.

NOMENCLATURE

c, constant;

d, channel width of the Hele-Shaw cell;

∇, $= (\frac{\partial}{\partial x}, \frac{\partial}{\partial y}, \frac{\partial}{\partial z})$;

∇_1^2, $= (\frac{\partial^2}{\partial x^2} + \frac{\partial^2}{\partial y^2})$;

g, acceleration of gravity;

h, height of the Hele-Shaw cell;

$\vec{i}, \vec{j}, \vec{k}$, unit vectors;

k_{HS}, permeability $\frac{d^3}{12Y}$;

N, truncation parameter;

Nu, Nusselt number;

p, pressure;

R_{HS}, Rayleigh number $\frac{\gamma g h \Delta T d^3}{\kappa_m \nu 12Y}$;

T, temperature;

ΔT, temperature difference between lower and upper boundary;

$\vec{v}$, $= (u,v,w)$ velocity vector;

x,y,z, Cartesian coordinates;

Y, full width of the Hele-Shaw cell (wall + channel);

GREEK LETTERS

α, wave number;

γ, coefficient of thermal expansion;

θ, temperature;

κ, thermal diffusivity;

ν, kinematic viscosity;

ρ, density;

SUBSCRIPTS

c, critical;

m, solid-fluid mixture;

o, reference values;

s, stationary values;

1 Introduction

During the recent years convection in a porous medium has received considerable interest, due both to its geophysical importance and to the mathematical simplicity of the model. A number of theoretical and experimental papers have appeared in the literature. Schneider [1], Elder [2], Buretta [3] and Bories & Combarnous [4] have performed laboratory experiments. Finite amplitude convection in a porous medium has been analysed numerically by Elder [2], Straus [5] and Kvernvold [6], and analytically by Palm, Weber & Kvernvold [7].

The analogy between motion in a porous medium and motion in a Hele-Shaw cell has frequently been used to simulate porous convection, especially with emphasis on the velocity distribution and the cell structure of the convective motion. See for example Wooding [8], Horne & O'Sullivan [9] and Hartline & Lister [10].

By defining an appropriate permeability the analogy between the stationary two-dimensional motion in a porous medium and the motion in a Hele-Shaw cell is obvious. However, one must be careful to use this similarity too far, because the stability properties for the two types of non-linear motion are quite different. In a porous medium disturbances of three-dimensional character are the most critical ones ([5], [6]) while for a Hele-Shaw cell only two-dimensional disturbances may exist.

The main aim of the present paper is to study the difference between the stability regions for non-linear convection in a Hele-Shaw cell and non-linear convection in a porous medium. Further, the velocity distribution and the heat transport are also discussed.

2 The governing equations

We consider a Hele-Shaw cell defined by two vertical planes of infinite horizontal extent, height h, and separated by a distance d, where $d \ll h$. The fluid confined in the cell is supposed to be bounded vertically by two perfect heat conducting and impermeable planes, having constant temperature T_1 and $T_1 + \Delta T$, respectively, where the lower plane is the warmer.

Following Hartline & Lister [10], the governing equations for motion in a Hele-Shaw cell may be written :

$$\vec{v} = -\frac{d^2}{12\mu}(\nabla p - \rho_0 \gamma g \theta \vec{k}) \tag{2.1}$$

$$\nabla \cdot \vec{v} = 0 \tag{2.2}$$

$$c\,\frac{\partial T}{\partial t} + \vec{v}\cdot\nabla T = \frac{Y}{d}\,\kappa_m \nabla^2 \theta \tag{2.3}$$

$$T = T_0 - \frac{\Delta T}{h}\,z + \theta \tag{2.4}$$

where the Boussinesque approximation has been utilized.

By introducing dimensionless quantities

$$h,\ \frac{\kappa_m Y}{hd},\ \Delta T,\ \frac{hd^3}{12\kappa_m \nu Y},\ c\,\frac{dh^2}{\kappa Y} \tag{2.5}$$

for length, velocity, temperature, pressure and time, respectively, the equations (2.1)-(2.4) becomes

$$\vec{v} = -\nabla p + R_{HS}\theta\vec{k} \tag{2.6}$$

$$\nabla \cdot \vec{v} = 0 \tag{2.7}$$

$$\frac{\partial \theta}{\partial t} + \vec{v}\cdot\nabla\theta = w + \nabla^2\theta \tag{2.8}$$

where the Hele-Shaw Rayleigh number is

$$R_{HS} = \frac{\gamma g \Delta T h d^3}{\kappa_m \nu 12 Y} \tag{2.9}$$

Equations (2.6), (2.7) and (2.8) are formally identical to the equations describing convection in a porous medium if the permeability for the Hele-Shaw cell is defined as

$$k_{HS} = \frac{d^3}{12Y} \tag{2.10}$$

The boundary conditions imposed on the system are

$$\theta = w = 0 \quad \text{for} \quad z = 0,1 \tag{2.11}$$

From equation (2.6) we observe that the vertical component of vorticity is zero. This, together with equation (2.7), makes it possible to introduce a scalar function, ψ, such that

$$\vec{v} = \nabla \times \nabla \times \vec{k}\psi = \vec{\delta}\psi \tag{2.12}$$

Further, by eliminating the pressure from equation (2.6), we find

$$\theta = -\frac{1}{R_{HS}} \nabla^2\psi \tag{2.13}$$

and by combining (2.6), (2.8), (2.12) and (2.13), we finally obtain

$$-\frac{\partial}{\partial t} \nabla^2\psi + \nabla^4\psi + R_{HS}\nabla_1{}^2\psi = \vec{\delta}\psi \cdot \nabla\nabla^2\psi \tag{2.14}$$

with the boundary conditions

$$\psi = \psi_{zz} = 0 \quad \text{for} \quad z = 0,1 \tag{2.15}$$

The critical Rayleigh number, R_{HSc}, is obtained from the linearized version of (2.14), giving $R_{HSc} = 4\pi^2$ for a critical wave number $\alpha_c = \pi$, where α is the overall horizontal wave number defined by $\nabla_1{}^2\psi = -\alpha^2\psi$. (Lapwood [11]).

3 Method of solution

To obtain a sufficiently exact solution of the problem for supercritical Rayleigh numbers the equations will be solved by numerical methods. Using Galerkin's method we will find a stationary solution of (2.14) and examine the stability of this solution with respect to small disturbances.

The stationary two-dimensional solution of (2.14) subject to the boundary condition (2.15) is obtained by expanding the function ψ in an infinite series :

$$\psi = \sum_{p=-\infty}^{\infty} \sum_{q=1}^{\infty} A_{pq} e^{ip\alpha y} \sin q\pi z \tag{3.1}$$

where each term satisfies the boundary conditions. The symmetry of the problem implies the restriction

$$A_{pq} = A_{-pq} \tag{3.2}$$

corresponding to convection cells without tilt.

Substituting (3.1) into (2.14), multiplying by $e^{-in\alpha x} \sin m\pi z$ and integrating over the whole fluid layer, we obtain an infinite set of algebraic equations for A_{nm} (Kvernvold [6])

$$\begin{aligned}&((n^2\alpha^2+m^2\pi^2)^2-Ra_{HS}n^2\alpha^2)A_{nm}\\ &=-\tfrac{1}{2}\sum_{k,l} A_{n-k,m+l}A_{kl}(k^2\alpha^2+l^2\pi^2)(km+ln)(n-k)\alpha^2\pi\\ &+\tfrac{1}{2}\sum s_{m,l}A_{n-k,s_{m,l}}(m-l)A_{kl}(k^2\alpha^2+l^2\pi^2)(km-ln)(n-k)\alpha^2\pi\end{aligned} \tag{3.3}$$

where

$$S_{m,l} = \begin{cases} 1 & \text{for } m > l \\ 0 & \text{for } m = l \\ -1 & \text{for } m < l \end{cases}$$

In order to handle this set it is necessary to truncate the series (3.1). We choose to neglect all terms with

$$|n| + \frac{m+1}{2} > N \tag{3.4}$$

where N is a sufficient large number.

Because of the symmetry of equation (2.14) the solution will only contain amplitudes with $n+m$ even, giving $N(N+1)/2$ equations to solve. For a given N the equations are solved by a Newton-Raphson iteration procedure. Usually less than 5 iterations are needed to obtain a satisfactorily convergent solution. To determine the value of the truncation parameter, N, we follow Busse [12] assuming the solution to be sufficiently accurate if, by replacing N by $N+1$, the Nusselt number

$$Nu = 1 - (\frac{\partial \bar{\theta}}{\partial t})_{z=0} \tag{3.5}$$

varies less than 1%. The over-bar denotes horizontal average.

After obtaining a solution, ψ_s, of the stationary set of equations (3.3), the stability of this solution with respect to infinitesimal disturbances is examined. By introducing $\psi = \psi_s + \psi'$ into equation (2.14) and linearize with respect to the infinitesimal disturbanc, ψ', we obtain the following equation

$$(\nabla_1^2 - \frac{\partial}{\partial t})\nabla^2\psi' + R_{HS}\nabla_1^2\psi' = \vec{\delta}\psi' \cdot \nabla\nabla^2\psi_s + \vec{\delta}\psi_s \cdot \nabla\nabla^2\psi' \tag{3.6}$$

with boundary conditions

$$\psi' = \psi'_{zz} = 0 \qquad \text{for} \qquad z = 0,1 \tag{3.7}$$

If there exists a solution of (3.6) with growing time dependence, the stationary solution is said to be unstable. Otherwise

is is stable.

A general expression for the perturbation, ψ', is given by

$$\psi' = \sum_{p,q} A_{pq} e^{ip\alpha x} e^{i(dx+by)+\sigma t} \sin m\pi z \qquad (3.8)$$

where d and b are free parameters. For a Hele-Shaw cell the geometry forces the motion to be purely two-dimensional, and consequently we may put b = 0. This means that the perturbation is two-dimensional with axis parallel to the axis of the stationary solution. Instability arising from disturbances of this type, is termed Eckhaus instability. For ordinary porous convection it may be shown that disturbances with d = 0 and b ≠ 0 are the most dangerous (Straus [5], Kvernvold [6]).

4 Results and discussions

The results of the numerical calculations are shown in Fig. 1 - 6. In Fig. 1 we have displayed the vertical heat transport defined by the Nusselt number (3.5) as a function of the Rayleigh number. It is assumed that there is no heat flux through the vertical walls of the Hele-Shaw cell. This may be achieved either by insulating the vertical walls, or by putting several Hele-Shaw cells beside each other. A medium composed of several Hele-Shaw cells (eventually with perforated, permeable walls) may also be treated as an anisotropic porous medium (Kvernvold & Tyvand [13]). The shaded area in Fig. 1 indicates the region for experimental results obtained by [1], [2] and [3].

In Fig. 2 we have shown the stability region for convection in a Hele-Shaw cell compared to the stability region for convection in a porous medium. We observe that convection in a Hele-Shaw cell is stable for a much wider range of wave numbers and Rayleigh numbers than ordinary porous convection. The stability region for two-dimensional convection in porous medium closes for $Ra \sim 8Ra_c$. For convection in a Hele-Shaw cell, however, the stability region did not show any tendency to close as far as calculations were performed.

The difference in the stability regions for convection in a porous medium and convection in a Hele-Shaw cell is a result of the different geometrical configurations of the two problems. While, for convection in a porous medium disturbances with arbitrary orientation will exist, the geometry forces the disturbances to be purely two-dimensional with axis parallel to the axis of the stationary roll for convection in a Hele-Shaw cell. For porous

convection the most unstable disturbances are of cross-roll character ($d = 0$) and have exponential time dependence. For a Hele-Shaw cell, however, only disturbances with $d = 0$ (Eckhaus-instability) exist, and the instability is of exponential character except for $\alpha < \alpha_c$ and $R_{HS} < 7.8\, R_{HSc}$, where it is oscillatory.

The results given in Fig. 2 confirm the results obtained by Horne & O'Sullivan [9] by a finite two-dimensional method. They found, by considering a unicelluar motion near the critical point and then by increasing the Rayleigh number slowly, that the motion became unstable for $R_{HS} \sim 7\, R_{HSc}$. From Fig. 2 we observe that cells with critical wavelength become unstable at $Ra_{HS} \sim 7.5\, R_{HSc}$. Further [9] found that, by suddenly raising the temperature difference between the boundaries, motion with shorter wavelength would occur and this motion was stable for Rayleigh numbers up to at least 1250. This is also seen from Fig. 2 where rolls with wave-numbers greater than $2\,\alpha_c$ are shown to be stable for Rayleigh numbers up to 500. No calculations have been performed for Rayleigh numbers above this value, but as mentioned before, there is nothing which indicates a closure of the stability region for even higher Rayleigh numbers.

We may therefore conclude from Fig. 2 that although the stationary motion in a Hele-Shaw cell and a porous medium are ~~analogous, the stability domains are quite different. This must~~ be taken into account when a Hele-Shaw cell is used to simulate porous convection.

Recent experimental investigators on convection in a Hele-Shaw cell ([9],[10]) have mainly been concerned with the velocity distribution and the cell structure. In Fig. 3 we have displayed

the calculated maximum value of the vertical velocity component for $\alpha = \alpha_c$. For comparison we have also plotted experimental values obtained by Hartline & Lister [10]. The figure shows satisfactory agreement between the analysis and the experiments. The numerical values lie in fact within the reported errorbounds for the measurements. The slightly trend, however, for the experimental values to lie somewhat below the numerical ones may perhaps be explained by looking at Fig. 4, where we have plotted the vertical velocity distribution for different values of the Rayleigh numbers. Fig. 4 shows that the vertical velocity is not symmetric about $z = \frac{1}{2}$, while [10] did assume symmetry in their handling of the experimental data. For experimental reasons they did not measure the vertical velocity component, w_m, at $z = \frac{1}{2}$, but at a distance away from this midline depending on the flow velocity. (Unfortunately, they do not give any values for this distance). The raw velocity data, w_m, are then adjusted to the midline velocity by assuming

$$w(z) = w_m \sin \pi z \tag{4.1}$$

The numerical results given in Fig. 4 shows that this last assumption is not a good approximation for R_{HS} greater than 2 - 2.5 times the critical Rayleigh number. For $R_{HS} < 2.5\, R_{HSc}$, however, where the flow is approximately symmetric about $z = \frac{1}{2}$, Fig. 3 shows that numerical and experimental results fit well together.

It is also worth mentioning the difference in the boundary conditions for the numerical and experimental model. In the experimental model the velocity vanishes identically at $z = 0,1$, while in the numerical model the velocity has its maximum value at the boundary. Although we would expect the boundary layer to be

of the same order of magnitude as the thickness of the Hele-Shaw cell, this will imply a horizontal volume flux which is from 5 to 10 percent lower in the experiments than in the numerical model. From continuity reasons, then,we would expect a smaller experimental value for the vertical velocity than those obtained by numerical methods.

In addition the velocity will also vary with the wave number. This is shown in Fig. 5, where the maximum value of the vertical velocity component is given as a function of the wave number and for different values of the Rayleigh number. As seen from the figure, the maximum value of the vertical velocity always occurs for wave numbers greater than the critical one. The variation is, however, less than 10 percent for wave numbers in the central region of the stability domain.

In Fig. 6 we have displayed some of the most important amplitudes, A_{nm}, for $\alpha = \alpha_c$ as functions of $\Delta R_{HS}/\Delta R_{HSc} = (R_{HS} - R_{HSc})/R_{HSc} = \Delta R$. The most striking features is the linear relation between the logarithms of the amplitudes and ΔR. This means that

$$A_{nm} \sim (\Delta R)^p \qquad (4.2)$$

In the paper by Palm, Weber and Kvernvold [7] it is found that for small ΔR $A_{11} \sim (\Delta R)^{0.5}$ and $A_{02} \sim \Delta R$. For larger overcritical Rayleigh numbers higher order of ΔR must be taken into account. From Fig. 6 we observe that $A_{11} \sim (\Delta R)^{0.57}$ for $\Delta R > 0.3$. For $\Delta R < 0.3$ numerical calculations show that p decreases and approaches 0.5 when $\Delta R \to 0$. Similarly, it is found that $A_{02} \sim (\Delta R)^{1.03}$ and $A_{04} \sim (\Delta R)^{1.5}$ for all ΔR greater than 0.1. (As far as two-dimensional motion is stable). The other

amplitudes shown in the figure can not be given by (4.2) only, but as a good approximation we may write

$$A_{31} \sim (\Delta R)^{1.5}, \quad A_{22} \sim (\Delta R)^{1.25} \quad \text{and} \quad A_{13} \sim (\Delta R)^{1.20}.$$

From an experimental point of view it would be of interest to verify this numerical results by a spectral analysis of the velocity field and the temperature field.

References

1 K.J. Schneider, Investigation of the influence of free thermal convection on heat transfer through granular materials. 11th Int.Cong.of Refrigeration, Munich (1963)

2 J.W. Elder, Steady porous convection in a porous medium heated from below. J.Fluid Mech. 27, 29-48 (1967)

3 R. Buretta, Thermal convection in a fluid filled porous layer with uniform internal heat sources. Ph.D. Dissertation, Univ. of Minnesota. (1972)

4 S.A. Bories & M.A. Combarnous, Natural convection in a sloping porous layer. J.Fluid Mech. 57, 63-79 (1973)

5 J.M. Straus, Large amplitude convection in a porous medium. J.Fluid Mech. 64, 51-63 (1974)

6 O. Kvernvold, Non-linear convection in a porous medium. Inst.Math., Univ. of Oslo, Preprint Ser.No.1 (1975)

7 E. Palm, J.E. Weber & O. Kvernvold, On steady convection in a porous medium, J.Fluid Mech. 54, 153-161 (1972)

8 R.A. Wooding, Instability of a viscous liquid of variable density in a vertical Hele-Shaw cell. J.Fluid Mech. 7, 501-515 (1960)

9 R.N. Horne & M.J. O'Sullivan, Oscillatory convection in a porous medium heated from below. J.Fluid Mech. 66, 339-352 (1974)

10 B.K. Hartline & C.R.B. Lister, Thermal convection in a Hele-Shaw cell. J.Fluid Mech. 79, 379-391 (1977)

11 E.R. Lapwood, Convection of a fluid in a porous medium. Proc. Camb. Phil. Soc. 44, 508-521 (1948)

12 F.H. Busse, On the stability of two-dimensional convection in a layer heated from below. J.Math.Phys. 46, 140-150 (1967)

13 O. Kvernvold & P.A. Tyvand, Nonlinear thermal convection in anisotropic porous media. Inst.Math., Univ. of Oslo, Preprint Ser. No. 2 (1977)

Figure legends

Figure 1 Nusselt number versus Rayleigh number

——— numerical values

shaded area; experimental values

Figure 2 Region of stable rolls

——•—— marginal stability

——— exponential instability

------- oscillatory instability

Figure 3 The maximum value of the non-dimensional vertical velocity for $\alpha = \alpha_c$ versus Rayleigh number

——— numerical values

▲ experimental values obtained by Hartline & Lister [10]

Figure 4 The variation of non-dimensional vertical velocity with height for $\alpha = \alpha_c$

Figure 5 The variation of the maximum value of the non-dimensional vertical velocity with wave number

Figure 6 The amplitudes, A_{nm}, versus $(R_{HS} - R_{HSc})/R_{HSc}$ for $\alpha = \alpha_c$

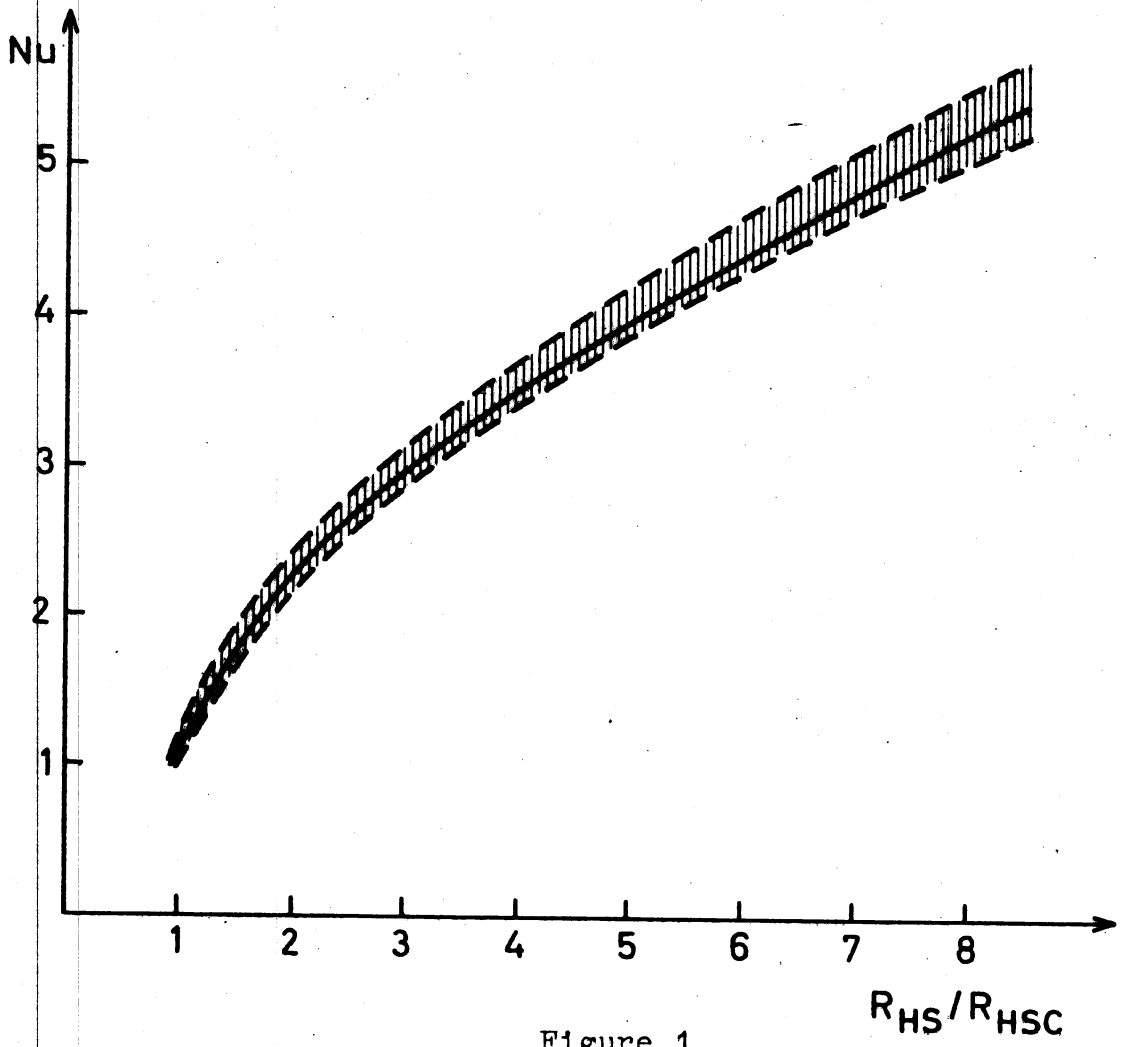

Figure 1

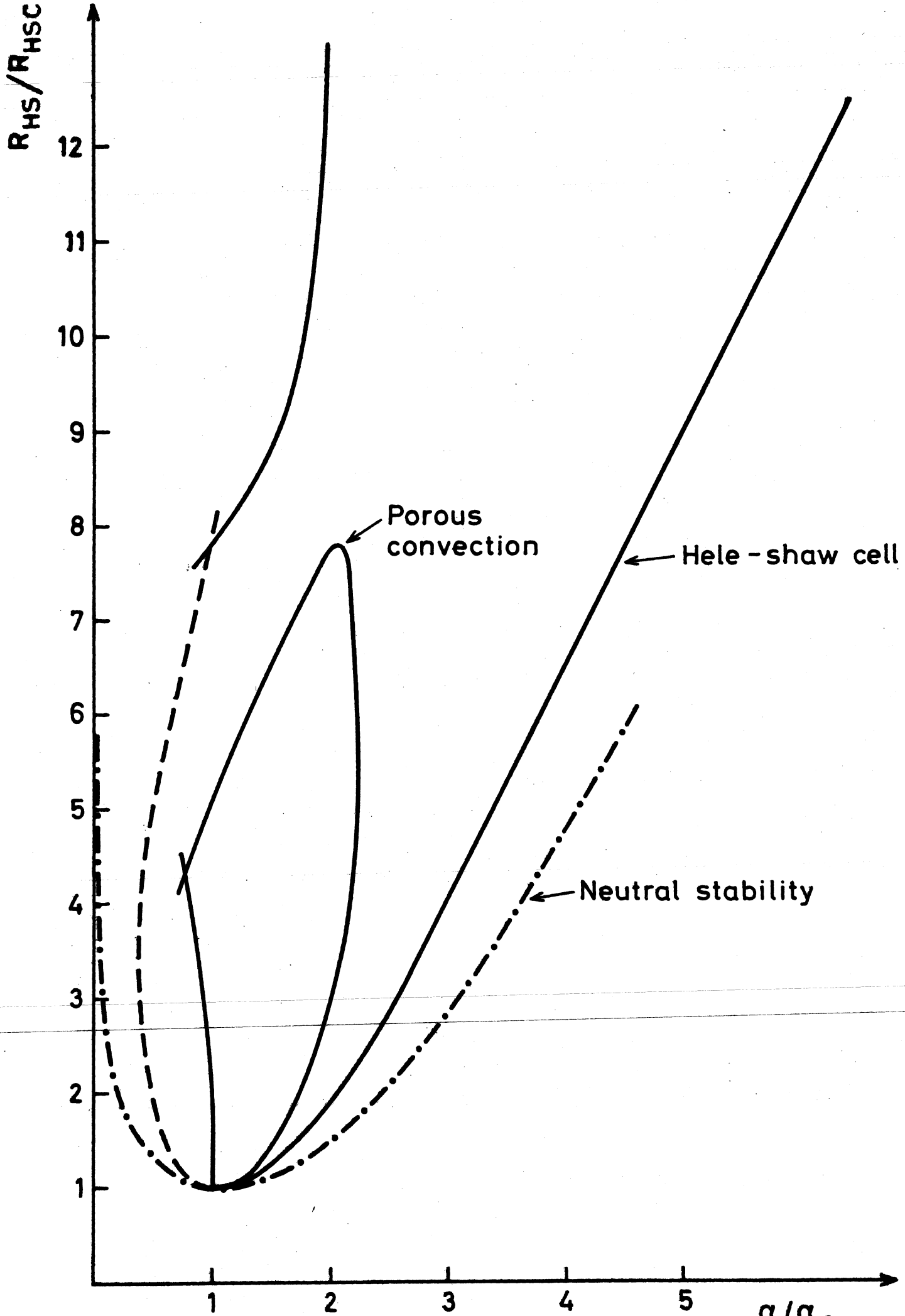
R_{HS}/R_{HSC}
12
11
10
9
8
7
6
5
4
3
2
1
Porous convection
Hele-shaw cell
Neutral stability
1
2
3
4
5
α/α_c

Figure 2

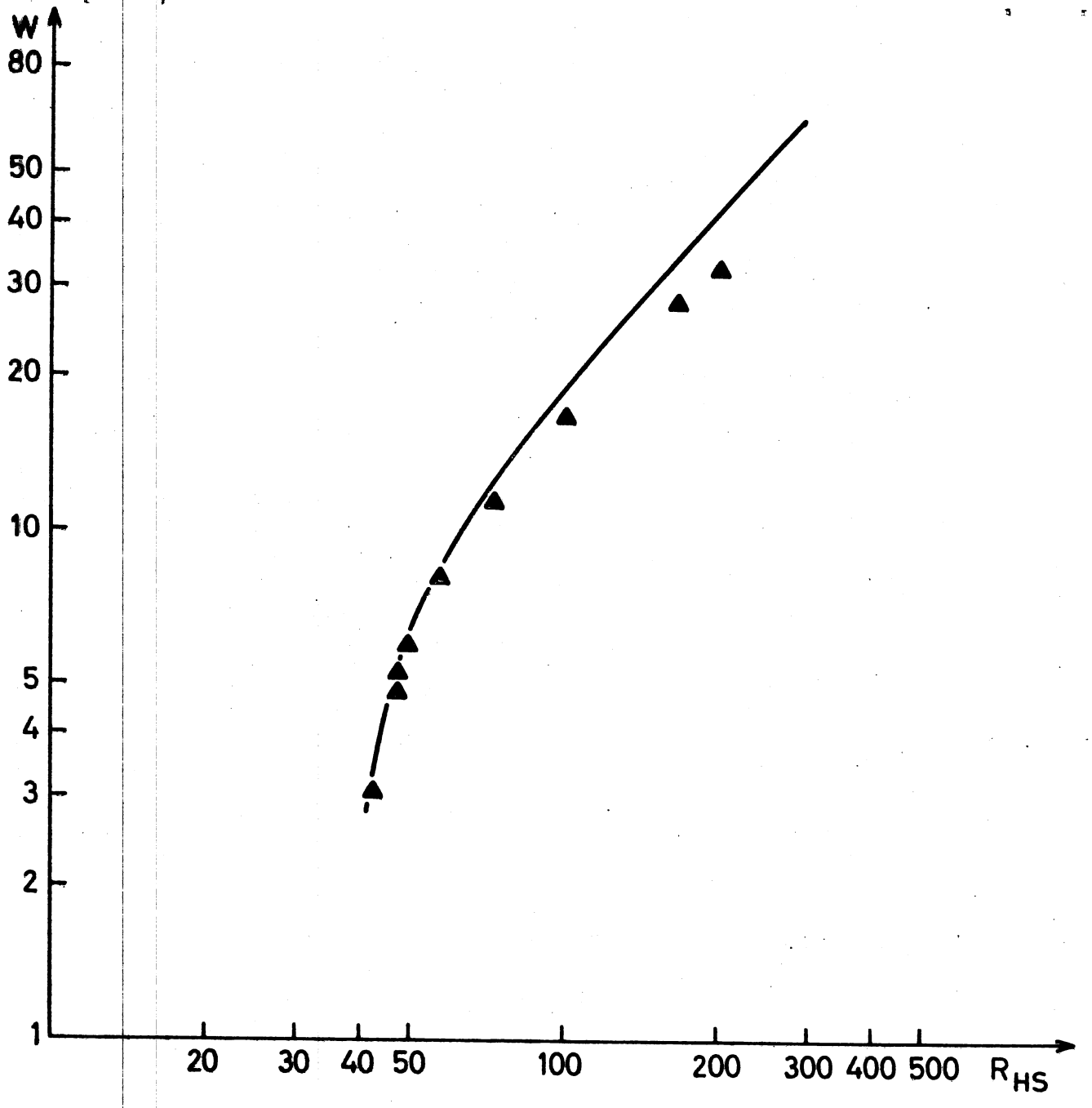

Figure 3

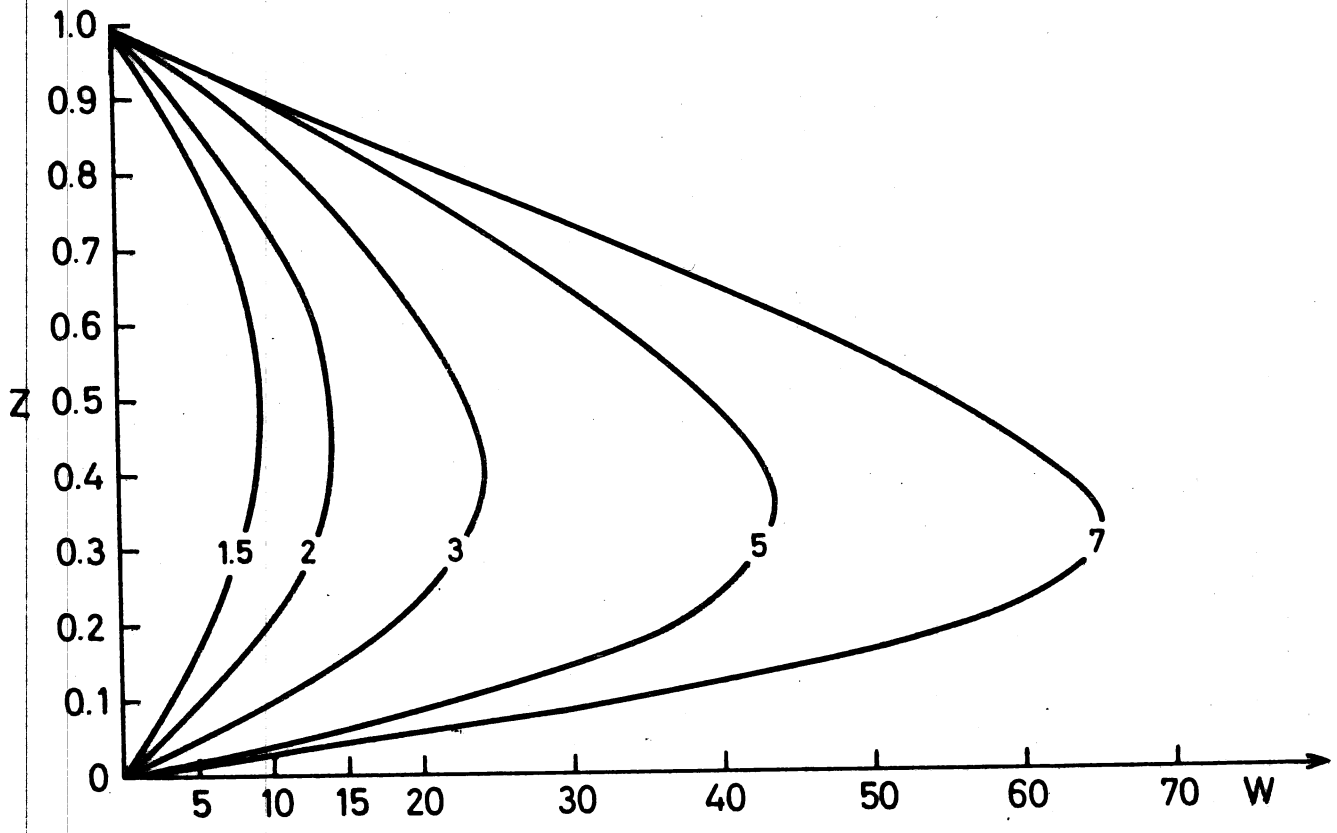

Figure 4

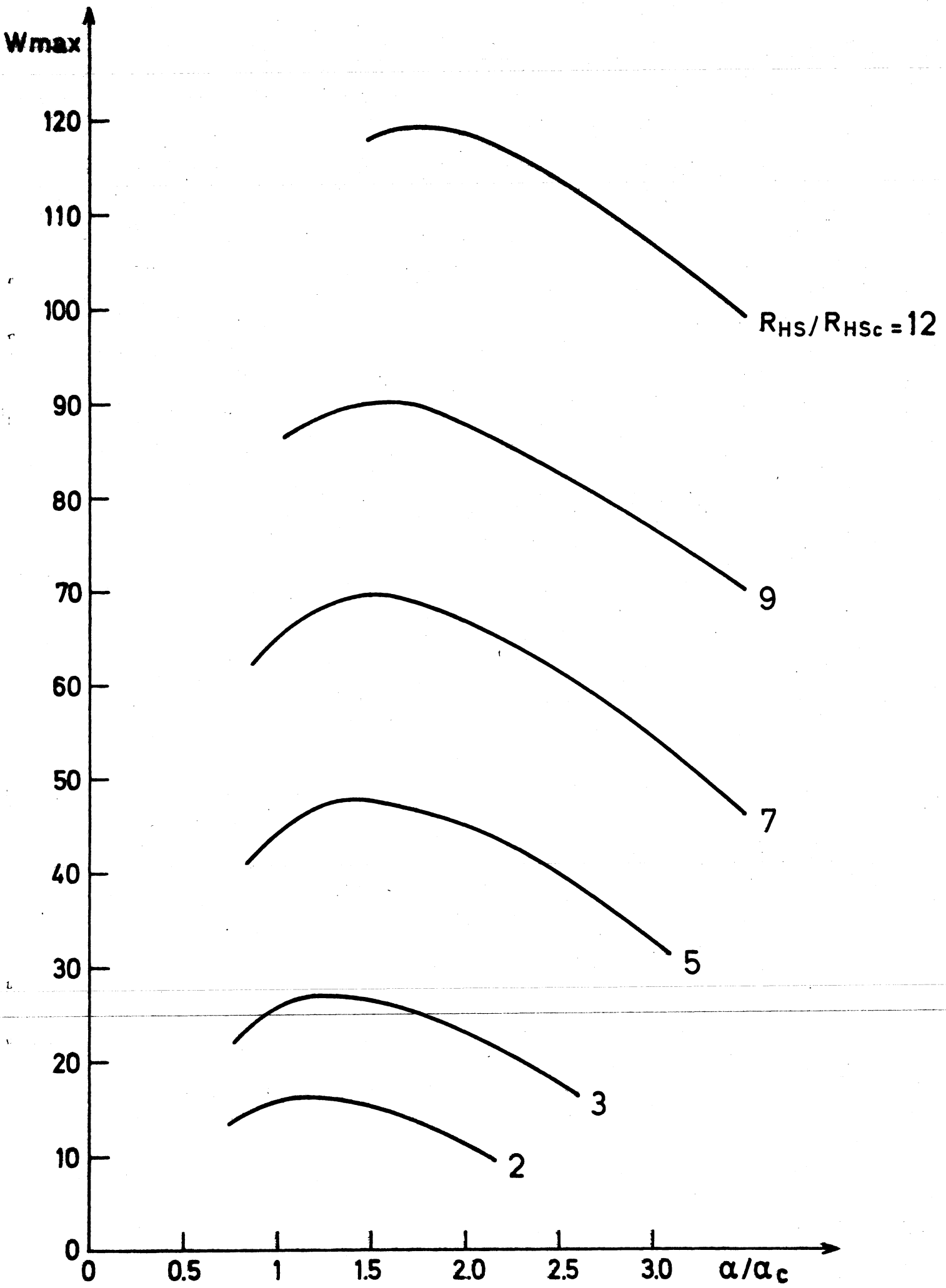
Wmax
120
110
100
90
80
70
60
50
40
30
20
10
0
0
0.5
1
1.5
2.0
2.5
3.0
α/αc
RHS/RHSc = 12
9
7
5
3
2

Figure 5

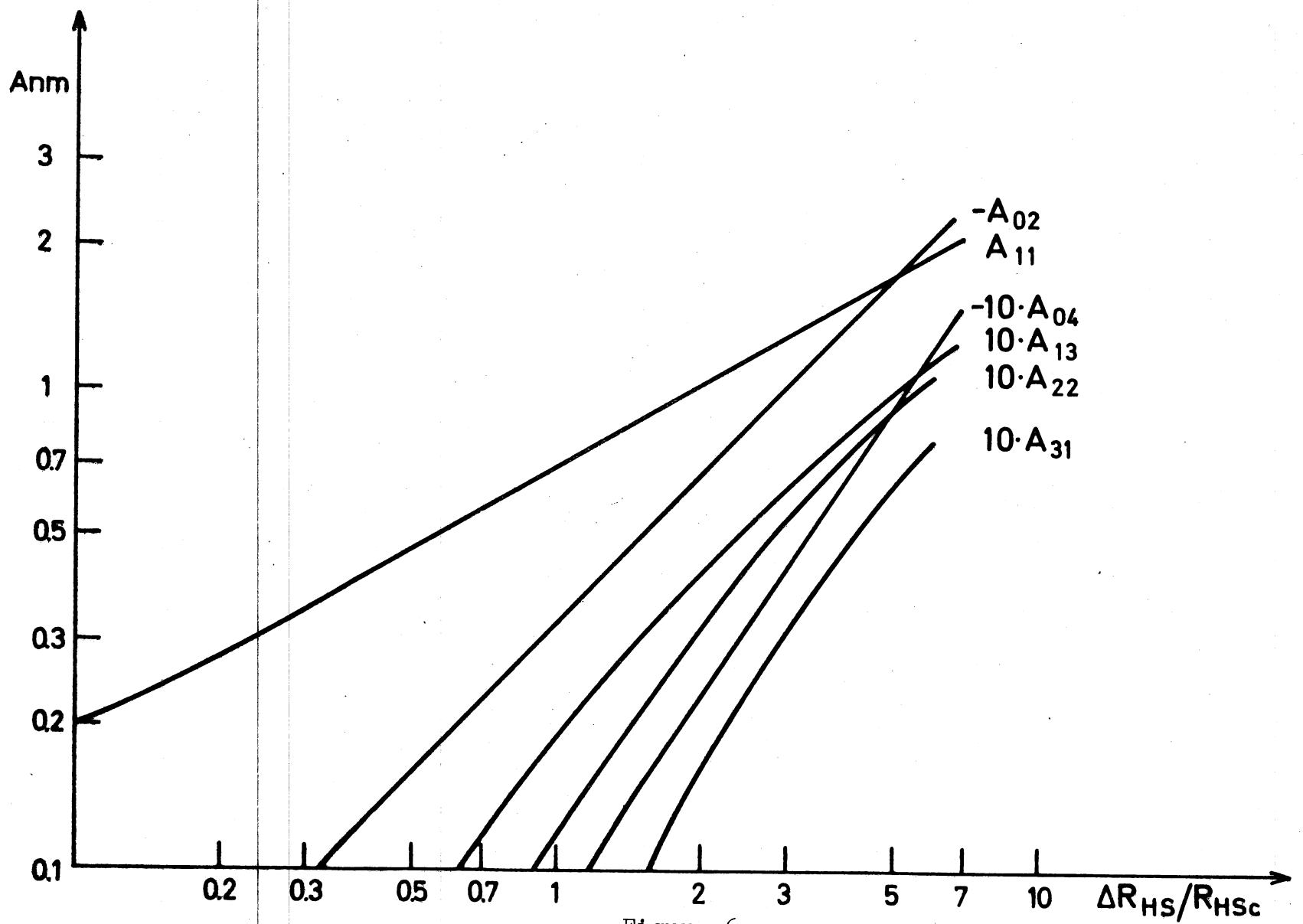
Anm
3
2
1
0.7
0.5
0.3
0.2
0.1
0.2
0.3
0.5
0.7
1
2
3
5
7
10
$\Delta R_{HS}/R_{HSc}$
$-A_{02}$
A_{11}
$-10 \cdot A_{04}$
$10 \cdot A_{13}$
$10 \cdot A_{22}$
$10 \cdot A_{31}$

Figure 6